Accuracy of the density-matrix renormalization-group method

Örs Legeza
Research Institute for Solid State Physics, H-1525 Budapest, P.O. Box 49, Hungary
and Technical University of Budapest, H-1521 Budapest, Hungary

Gábor Fáth*
Institute of Theoretical Physics, University of Lausanne, CH-1015 Lausanne, Switzerland
(Received 11 December 1995)

White's density-matrix renormalization-group (DMRG) method has been applied to the one-dimensional Ising model in a transverse field (ITF), in order to study the accuracy of the numerical algorithm. Due to the exact solubility of the ITF for any finite chain length, the errors introduced by the basis truncation procedure could have been directly analyzed. By computing different properties, like the energies of the low-lying levels or the ground-state one- and two-point correlation functions, we obtained a detailed picture of how these errors behave as functions of the various model and algorithm parameters. Our experience with the ITF contributes to a better understanding of the DMRG method, and may facilitate its optimization in other applications. [S0163-1829(96)05418-5]

I. INTRODUCTION

In the past three years we have witnessed a breakthrough in the numerical analysis of one-dimensional (1D) quantum lattice models. This considerable progress was due to the invention of the density-matrix renormalization-group (DMRG) method by White.[1] Recent applications of the method has demonstrated its extreme efficacity and versatility. By now the DMRG has become one of the leading numerical tools in the study of most 1D quantum spin and electron problems of current interest.

There are several numerical methods to obtain the low-energy states of a given quantum Hamiltonian. Exact diagonalization algorithms are able to compute the ground state and the lowest excited states with a precision of more than 12 digits. The attainable system sizes, however, are rather limited due to memory restrictions. On the other hand, stochastic methods, like the diverse variants of the quantum Monte Carlo method, are capable of treating systems with hundreds of sites — at the price of reducing the precision of the obtained results. In this case, it is rather the computation time that limits the applications. Use of renormalization-group procedures, such as the DMRG, could be the way out of this dilemma. The key idea is to gradually increase the system size, and, at the same time, systematically truncate the Hilbert space by keeping only those degrees of freedom that are really ''important'' for an accurate representation of the desired state. The main point, and this is where the DMRG differs drastically from the preceding numerical RG methods, is how to choose the most important degrees of freedom to minimize the error caused by discarding the other ''unimportant'' ones.

The DMRG is an iterative algorithm to build up the lattice to the desired length and find approximants to the target state (the ground state or an excited state), using only a limited number of basis states. The total system is divided into two parts, the block and the environment. In each step of the procedure the block is increased by adding one lattice site, but only the most probable states, obtained from the reduced density matrix of the block, are kept. The environment is composed from the block of the previous step, and its role is to embed the block into a larger system, when the density-matrix is formed. Application of the reduced density matrix in the truncation process, and not simply keeping the lowest energy states of the block as in previous RG techniques,[2] is the key ingredient of the DMRG method, since, as was shown by White,[1] this is the way to minimize the error introduced into the representation of the target state. Although, during the algorithm the length of the total system increases gradually, the dimension of the Hilbert space is always kept manageable by the truncation process, and systems with relatively large size can be studied.

The DMRG has been successfully applied to various 1D and coupled chain problems, such as $S=1/2$ (Refs. 1,3) and $S\geqslant 1$ (Ref. 4) spin chains, strongly correlated electron systems,[5] impurity problems,[6] or the two-chain Heisenberg and Hubbard models.[7] Promising implementations of the algorithm to compute dynamical properties[8] of 1D systems or to simulate 2D lattices[9,10] have also been reported. At least for quasi-1D problems, its advantage over the standard numerical procedures has become evident. While the available system sizes are comparable to those of the Monte Carlo method, the precision of the computed quantities seems better by several orders of magnitude.

The DMRG works especially well when the system is subject to open boundary condition. In the case of periodic boundary condition, on the other hand, errors are definitely stronger. Moreover, the conservation of momentum cannot be directly built into the method, so restriction of the computation to a certain momentum sector is not possible. These drawbacks have led to the fact that a large part of current applications of the method treat *open* systems.

Although this is a renormalization-group procedure, contrary to the naive expectations, results seem more accurate if the system is away from criticality, i.e., when the model possesses a finite spectral gap in the thermodynamic limit.

Other parameters of the model in study, like the number of degrees of freedom at a single site or the range of interactions also have drastic effects on the precision.

For any numerical method, it is of essential importance to understand, how errors evolve, when parameters of the procedure or those of the model in study are varied. So far, the accuracy of the DMRG method has only been tested on small clusters where numerically exact results were known from exact diagonalization, or alternatively, large lattice DMRG data were extrapolated to the infinite chain limit, and these extrapolated values have been compared to rigorous results, available only in the thermodynamic limit. In many of the applications, however, at most the small lattice exact data are available for testing. Nevertheless, large lattices, even with hundreds of sites, are used to draw conclusions on the behavior of the system. In many cases, it is really a difficult problem to reliably estimate the precision as the system size increases.

Our main goal in this paper is to study the general trends of numerical errors during the DMRG algorithm, especially when the length of the system is in the range of the typical applications, i.e., well beyond the limit where exact diagonalization data are attainable. For this purpose, we apply the method to an exactly solvable system, the *Ising model in a transverse field* (ITF). The main advantage of the ITF model as a test system is that its energy spectrum and ground-state correlation functions can be calculated by simple tools for *any finite* chain length, even when the chain is subject to *open* boundary condition, as in the standard DMRG applications. The ITF is also a model with a second order quantum phase transition, so the effect of the appearance of criticality on the accuracy can also be analyzed.

We carried out a detailed DMRG study of the ITF, varying several parameters of the model and the numerical procedure, like the strength of the magnetic field, the chain length, the number of states kept, the number of iterations and the number of target states. Beside the energies of the low-lying states, we also computed different one- and two-point correlation functions.

The setup of the paper is as follows. In Sec. II we briefly summarize the exact solution of the ITF with open boundary condition. Section III is devoted to the details of the DMRG algorithm, while Sec. IV contains the analysis of the observed trends in the numerical errors. Section V is a summary of our main conclusions.

II. THE 1D ITF WITH OPEN BOUNDARY CONDITION

The Ising model in a transverse field (ITF) on a one-dimensional chain of N sites is defined by the following Hamiltonian:

$$\mathscr{H}=-\sum_{n=1}^{N-1}\sigma_n^x\sigma_{n+1}^x-\gamma\sum_{n=1}^{N}\sigma_n^z, \tag{1}$$

where σ^α, $\alpha=x,y,z$ are the Pauli matrices, γ is the transverse magnetic field applied in the z direction, and the chain is subject to *open* boundary condition, as in our DMRG implementation.

In the thermodynamic limit, the ITF possesses a second order phase transition that takes place at $\gamma=1$, where the energy gap vanishes as $N\to\infty$. For $\gamma<1$ (ordered phase), the ground state is doubly degenerate and there is a long-range order: the ground-state correlation function $\rho_l^x=\langle\sigma_n^x\sigma_{n+l}^x\rangle$ tends to a finite value as $l\to\infty$. On the other hand, for $\gamma>1$ (disordered phase), the ground state is unique and $\rho_l^x\to 0$ as $l\to\infty$. The gap is finite on both sides of the transition point.

The ITF in Eq. (1) is exactly solvable for any chain length N. Details of the calculation can be found, e.g., in Ref. 11. Here we only summarize the main steps and the necessary formulas. Introducing Fermi operators via the Jordan-Wigner transformation

$$c_n=\exp\left(\pi i\sum_{j=1}^{n-1}\sigma_j^+\sigma_j^-\right)\sigma_n^-, \tag{2}$$

the Hamiltonian $\mathscr{H}$ reduces to a quadratic form

$$\mathscr{H}=-2\gamma\sum_{n=1}^{N}c_n^\dagger c_n-\sum_{n=1}^{N-1}(c_n^\dagger c_{n+1}+c_n^\dagger c_{n+1}^\dagger+\text{H.c.})+N\gamma. \tag{3}$$

This can be diagonalized directly by a Bogoliubov transformation[12]

$$\eta_k=\sum_{n=1}^{N}\left(\frac{\phi_n^k+\psi_n^k}{2}c_n+\frac{\phi_n^k-\psi_n^k}{2}c_n^\dagger\right), \tag{4}$$

leading to the final diagonal form

$$\mathscr{H}=\sum_{k\ \text{allowed}}\Lambda(k)\left(\eta_k^\dagger\eta_k-\frac{1}{2}\right), \tag{5}$$

$$\Lambda(k)=2(1+\gamma^2+2\gamma\cos k)^{1/2}. \tag{6}$$

The N-element real vector ϕ^k is a solution of a set of linear equations,[11] and turns out to be

$$\phi_n^k=A_N\left(\sin kn-\frac{\sin k}{\gamma+\cos k}\cos kn\right), \tag{7}$$

where $n=1,2,\ldots,N$ and A_N is a normalization constant. ψ^k can be expressed from ϕ^k as

$$\psi_n^k=A_N'(\gamma\phi_n^k+\phi_{n+1}^k), \tag{8}$$

where A_N' is another normalization constant, and formally $\phi_{N+1}^k\equiv 0$.

Reflecting the fact that the chain is subject to open boundary condition, the allowed k modes in the summation of Eq. (5) cannot be written in a simple form for general γ, but are determined through a trigonometric equation

$$\frac{\sin[k(N+1)]}{\sin(kN)}=-\frac{1}{\gamma}. \tag{9}$$

In any case, the total number of independent modes is equal to the number of sites N. By convention, the allowed k values are the roots $k=k_0+ik_1$, whose real part k_0 is in the interval $0<k_0\leq\pi$. When $\gamma>\gamma_c(N)\equiv N/(N+1)$ all the roots are real. For $\gamma<\gamma_c(N)$, however, a complex (*localized*) solution becomes possible with $k_0=\pi$ and $k_1>0$. Note

that $\gamma_c(N)\to\gamma_c=1$, the phase transition point, as $N\to\infty$. The imaginary part k_1 can be obtained by solving the equation

$$\frac{\sinh[k_1(N+1)]}{\sinh(k_1N)}=\frac{1}{\gamma}, \tag{10}$$

and the corresponding ϕ vector is[11]

$$\phi_n^{\rm loc}=A_N(-1)^{n-1}\sinh[(N-n+1)k_1], \tag{11}$$

where, again, $n=1,2,\ldots,N$ and A_N is a normalization constant. $\psi_n^{\rm loc}$ is obtained again through Eq. (8). The elements of $\phi_n^{\rm loc}$ and $\psi_n^{\rm loc}$ are exponentially small far from the left and right chain ends, respectively, which indicates, by Eqs. (4), that the complex mode is localized to the chain ends. The energy associated with this localized mode is

$$\Lambda(\pi+ik_1)=2(1+\gamma^2-2\gamma\cosh k_1)^{1/2}. \tag{12}$$

When N is large, Eq. (10) is readily solved to yield $k_1\sim\ln 1/\gamma$. By substitution, this gives $\Lambda(\pi+ik_1)\sim 0$, i.e., it is a mode of zero energy, leading to the double degeneracy of the ground state sector when $\gamma<1$.

The ground state energy of the model, the fermionic vacuum, is expressed as

$$E_0=\frac{1}{2}\sum_{k\ \text{allowed}}\Lambda(k), \tag{13}$$

that can be written in a closed form only at the transition point $\gamma=1$, where it reduces[13] to

$$E_0=1-\ \text{cosec}\left(\frac{\pi}{4N+2}\right). \tag{14}$$

The first excited state of the model is always determined by the wave number k, whose real part k_0 is closest to π; for $\gamma>\gamma_c$ it is a real root and the energy gap converges to $2(\gamma-1)$ as $N\to\infty$. For $\gamma<\gamma_c$, this is the localized mode, and the first excited state becomes asymptotically degenerate with the ground state. It is the second excited state that constitute the real (finite) energy gap in this case.

Finally, ground-state one- and two-point correlation functions can also be calculated, by the method described in details by Lieb *et al.*[12] The only interesting one-point function is $\mathscr{M}_n^z=\langle\sigma_n^z\rangle$, which can be expressed as

$$\mathscr{M}_n^z=\frac{1}{2}G_{nn}, \tag{15}$$

where G_{nm} is defined by

$$G_{nm}=-\sum_{k\ \text{allowed}}\psi_n^k\phi_m^k. \tag{16}$$

Note that even in the ordered state $\mathscr{M}_n^x=\langle\sigma_n^x\rangle=0$, since the Hamiltonian, and thus any finite lattice ground state, is invariant to the transformation $\sigma_n^x\to-\sigma_n^x$. The same holds for σ_n^y, so that $\mathscr{M}_n^y=\langle\sigma_n^y\rangle=0$, too. As for the two-point functions, $\rho_{nm}^x=\langle\sigma_n^x\sigma_m^x\rangle$, $\rho_{nm}^y=\langle\sigma_n^y\sigma_m^y\rangle$, and $\rho_{nm}^z=\langle\sigma_n^z\sigma_m^z\rangle$, one arrives to the formulas

$$\rho_{nm}^x=1/4\begin{vmatrix} G_{n,n+1} & G_{n,n+2} & \cdots & G_{nm}\\ \vdots & & & \vdots\\ G_{m-1,n+1} & \cdots & & G_{m-1,m}\end{vmatrix}, \tag{17}$$

$$\rho_{nm}^y=1/4\begin{vmatrix} G_{n+1,n} & G_{n+1,n+1} & \cdots & G_{n+1,m-1}\\ \vdots & & & \vdots\\ G_{m,n} & \cdots & & G_{m,m-1}\end{vmatrix}, \tag{18}$$

and

$$\rho_{nm}^z=1/4(G_{nn}G_{mm}-G_{mn}G_{nm}), \tag{19}$$

where $n<m$.

In order to be able to compare the approximate results, produced by the DMRG method, with the exact ones for a certain value of γ and chain length N, the exact quantities were calculated by an independent numerical process, using either double precision FORTRAN routines or the MATHEMATICA software that allows computations with arbitrary precision. We solved the nonlinear equations (9) and (10) to obtain the allowed set of wave numbers, and used these values to express the associated ϕ^k and ψ^k vectors. Then the ground-state and excited state energies and the correlation functions were calculated numerically according to the above formulas. All the results obtained in this way were precise to at least 14 digits.

III. THE DENSITY-MATRIX RENORMALIZATION-GROUP METHOD

White's density-matrix renormalization-group method (DMRG) is a numerical real-space renormalization-group procedure, in which the effective size of the system increases gradually, while the dimension of the associated Hilbert space remains constant, due to a systematic truncation process. Since the method is well described in the original papers,[1] we only present a brief summary here.

The basic object of the method is the system block B_l that consists of l lattice sites. All the necessary operators $\mathscr{O}_i$ of this block (e.g., σ_n^α, $\alpha=x,y,z$ and $1\leqslant n\leqslant l$) are stored as $M\times M$ matrices. Note that the real dimension of a block of l sites is d^l, where d is the number of states at a single site, and $M\ll d^l$, so the representation of the block matrices is only approximative. In each step of the algorithm, a new single site ● is added to the existing block B_l, and operators of the resulting system B_l● of dimension Md are formed as tensor products from the matrix representations of the corresponding operators of the two constituting parts. B_l● is then renormalized, first by carrying out an appropriate unitary transformation, then by truncating its degrees of freedom from Md to M. Only the most important M states are kept, and the remaining $M(d-1)$ ones are discarded. The resulting system of dimension M and length $l+1$, denoted by B_{l+1}, is then used iteratively in the subsequent step of the algorithm. Choosing the states kept, i.e., finding the appropriate unitary transformation, is the most crucial point of the renormalization-group procedure.

Previous applications of the renormalization-group technique, where the M lowest energy states of B_l● were kept,

led to disappointing results for many model systems. As was observed by several authors,[14] this was due to the interaction having been neglected during the renormalization process between $B_l\bullet$ and the rest of the larger (in many cases infinite) system of what it makes a part. $B_l\bullet$ was renormalized in a way that an unnatural open boundary condition was forced on both of its ends.

In order to avoid this problem, White's method embeds $B_l\bullet$ into a superblock, and uses the eigenstates of this larger system to carry out the renormalization of $B_l\bullet$. Choosing the superblock configuration as $B_l\bullet\bullet B_l^R$, where B_l^R is the reflection of B_l, its effective Hamiltonian, built up from the matrix representations of the necessary operators of the two blocks and the two single sites, is diagonalized to obtain the desired (target) state Ψ. Even though the target state can be a linear combination of more states, by targeting only one state, the renormalized block states are more specialized for representing that single one, and fewer of them are needed for a given accuracy.

Having the target state expressed on the superblock as

$$\Psi=\sum_{i,j=1}^{Md}\Psi_{i,j}|i\rangle|j\rangle, \tag{20}$$

where i and j label the Md states of $B_l\bullet$ and its surroundings $\bullet B_l^R$, respectively, the reduced density-matrix of the subsystem $B_l\bullet$ is formed as

$$\rho_{ii'}=\sum_j \Psi_{ij}\Psi_{i'j}. \tag{21}$$

As was shown by White,[1] the error introduced into the representation of the target state by the truncation to M states is minimized, if the new basis that one changes to is the basis that diagonalizes the density-matrix $\rho_{ii'}$. The renormalization of the tensor product operators of $B_l\bullet$,

$$\mathscr{A}_i\rightarrow\mathscr{O}\mathscr{A}_i\mathscr{O}^\dagger, \tag{22}$$

is thus carried out by the $M\times Md$ transformation matrix $\mathscr{O}$, whose rows are composed from the M density-matrix eigenvectors, associated to the M largest eigenvalues ω_α, $\alpha=1,\ldots,M$.

The simplest version of the DMRG method, the *infinite lattice algorithm*, starts with four lattice sites, i.e., from the superblock configuration $B_1\bullet\bullet B_1^R$. In each step, the total length of the chain increases by 2. Measurements of the interested quantities are made after the calculation of the target state in each step, and the whole process is continued until the results converge satisfactorily. This method is especially suitable to yield, with minimal computational efforts, rather precise estimates of bulk properties, like the ground-state energy density or ground-state correlation functions.

The usual measure of the accuracy of the truncation to M states is the deviation of the sum of the density-matrix eigenvalues associated with the states kept $P_M\equiv\Sigma_{\alpha=1}^M\omega_\alpha$ from unity. Clearly, in the extreme case when the discarded states have zero weight, i.e., $\omega_{M+1}=\omega_{M+2}=\cdots=\omega_{Md}=0$ so that $P_M=1$, they are not required to represent the target state Ψ, and no error has been committed. There is, however, another source of error in the DMRG procedure, namely that the $B_l\bullet$ subsystem is only embedded into an *approximate* superblock when it is renormalized, and not into the, *a priori* unknown, exact environment. The two kinds of errors, the ''truncation'' error and the ''environment'' error are not simply additive. The latter one, however, can be reduced in an iterative manner, using the so-called *finite lattice algorithm*.

The finite lattice algorithm starts by building up the lattice to the desired length N, using the infinite lattice algorithm. Then the superblock configuration is modified to $B_l\bullet\bullet B_{N-2-l}^R$, so that the total length remains always N, and the blocks B_l, $l=1,\ldots,N-3$, are recomputed. The process when all B_l's are recomputed constitute the *cycle* of the algorithm. Since at each step from this time on, the block to be renormalized is part of a system of the desired length N, the environment becomes more precise, and a considerable improvement of the results, corresponding to the N-site system, is achieved. These results can be then used to carry out a systematic finite-size scaling analysis, or to study, e.g., boundary effects in the finite chain.

IV. NUMERICAL RESULTS

In order to determine the accuracy of DMRG method, numerical calculations on the ITF, using both the infinite and finite lattice algorithms, were performed. Errors in various quantities, such as the ground-state and first excited-state energies E_{GS} and E_{1XS}, respectively, the one-point correlation functions $\mathscr{M}_n^z$ and $\mathscr{M}_n^x$, and the two-point correlation functions ρ_l^z and ρ_l^x were monitored. In the case of the *infinite* system algorithm, our main concern was how the errors of the energies depend on the system size N, when other parameters are kept constant. In the *finite* lattice algorithm, on the other hand, the length of the chain was kept fixed, and the effect of introducing additional cycles in the process was analyzed. When excited states were computed, the number of target states was also varied.

Since the ITF possesses a second order phase transition at $\gamma_c=1$, it was expected that many of the above quantities have different behavior, whether γ is equal to the critical value, or greater or less than γ_c. Therefore, we investigated the three different regions of the phase diagram by choosing three different values for γ, namely, $\gamma=0.5<\gamma_c$, $\gamma=1=\gamma_c$, and $\gamma=2>\gamma_c$.

A. Energies

Let us first consider the error of the ground-state (GS) and first excited-state (1XS) energies. Using the *infinite lattice algorithm*, we built up a chain of length $N=300$ and kept states up to $M=48$. Except one example which will be discussed below, we found that targeting one state alone is by orders of magnitude more precise than targeting several states together. Hence, unless stated otherwise, the results to be presented here were obtained in a way that the ground state and the first excited state were targeted *separately*.

The errors $E(\mathrm{DMRG})-E(\mathrm{exact})$ were always found to be positive, satisfying the statement that the DMRG is a variational method, which gives (at least for the GS energy) an upper bound estimate.[9] The relative errors $\delta E\equiv[E(\mathrm{DMRG})-E(\mathrm{exact})]/|E(\mathrm{exact})|$ as a function of N for various values of M and γ are shown on log-log scale in Figs. 1–3.

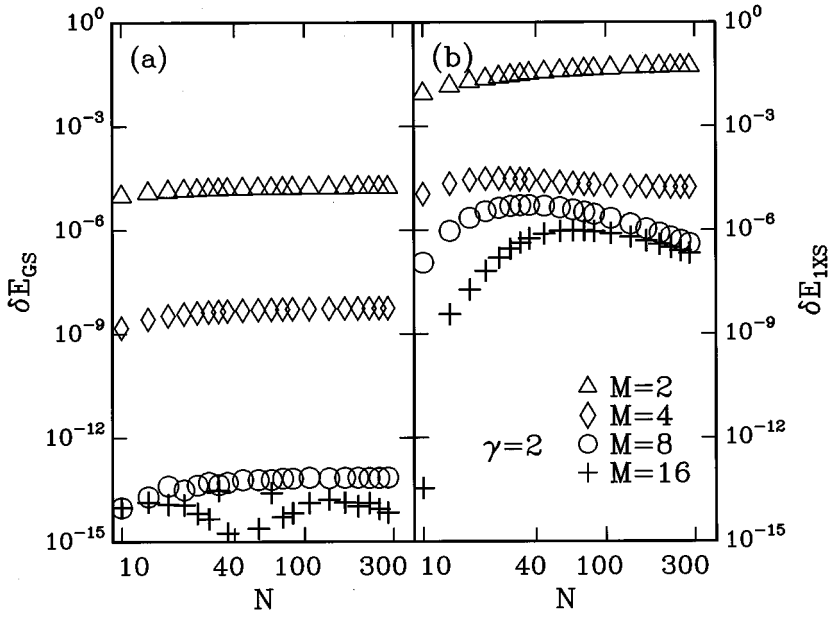

FIG. 1. Relative errors of the (a) ground-state energy, and (b) first excited-state energy as a function of the chain length N for different values of M. Data obtained by the infinite lattice algorithm ($I=1$) in the disordered regime at $\gamma=2$.

Until the algorithm keeps all states, i.e., for $N \leqslant 2(\ln M+1)$, the DMRG is exact and only the machine's numerical inaccuracy is seen, limiting the precision on the order of 10^{-14}. For longer chains, however, the errors associated with the reduction of degrees of freedom also come in.

For the off-critical values, $\gamma=2$ and 0.5, the ground-state error δE_{GS} shows practically no size dependence. It depends, however, crucially on the value of M. The behavior is the most clear for $\gamma=2$, where the infinite system ground state is unique with a gap above it. Even a small value of M, $M\sim 10$, is enough to reach the machine's precision limit [Fig. 1(a)]. There is, on the other hand, an interesting size dependence in the error of the first excited state $\delta E_{1\mathrm{XS}}$, especially for greater M values [Fig. 1(b)]. A maximum evolves, above which $\delta E_{1\mathrm{XS}}$ begins to dwindle again. This can be understood, however, since the approximate excited state, yielded by the DMRG process, is not necessarily exactly orthogonal to the real ground state, and can have a finite overlap with it. This fact leads to an overcompensation of the otherwise increasing positive absolute error for long chains.

For $\gamma=0.5$, where the ground state is asymptotically doubly degenerate, the behavior is more subtle [Figs. 2(a,b)]. The splitting of the two lowest levels decreases exponentially as N increases. When this difference goes below the machine's precision limit $\sim 10^{-14}$, the algorithm is incapable to further resolve the two levels, and the target state that it yields is a linear combination of the two exact eigenvectors with random coefficients. As a consequence, in each step of the DMRG algorithm the target state changes unpre-

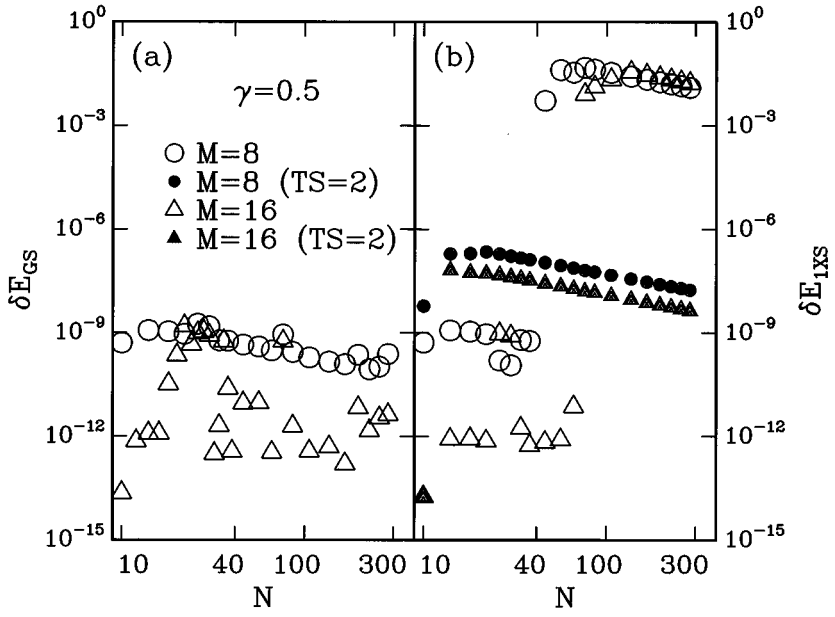

FIG. 2. Same as Fig. 1, but in the ordered regime at $\gamma=0.5$. Curves labeled by TS=2 show the case, when the excited state was targeted together with the ground state.

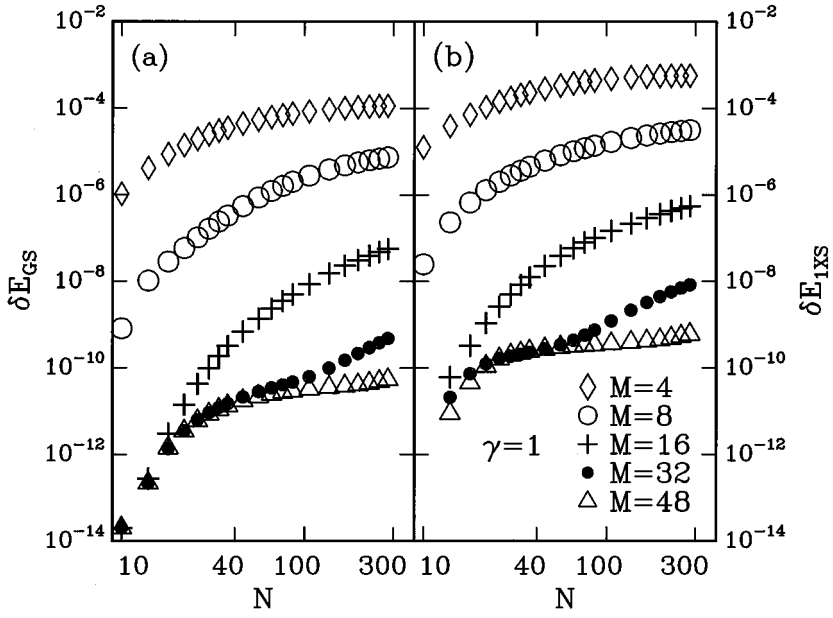

FIG. 3. Same as Fig. 1, but at the critical point $\gamma=1$. Curves with $M=4,8,16$ are dominated by the truncation error, while those with $M=48$ by the environment error. The $M=32$ curves show a crossover between the two types.

dictably, leading to the loss of optimality of the truncation process, and hence, to considerably higher, rather scattered error rates. As Fig. 2(b) shows, the DMRG can even ''lose'' the target state above a certain chain length. In a try to avoid these problems, we also computed E_{1XS} by choosing the target state to be a linear combination of the ground-state and the first excited-state vectors. This proved to be an improvement in the range where otherwise the excited state was lost; for smaller values of N, however, the errors were considerably larger [Fig. 2(b)].

At the critical point $\gamma=1$, the errors were found to be by several orders of magnitude larger than at the off-critical values of γ. This is in accordance with the findings of Ref. 15: the correlation length of the model is one of the most significant factors that influence the precision of the DMRG method. Moreover, the curves in Figs. 3(a,b) have a clear size dependence. When M is kept fixed, the errors can become larger by 4 to 6 orders of magnitude, as the chain length approaches $N=300$. For smaller M, the clear downward curvature seen in the log-log plot indicates that the errors converge to a finite value at large lengths. For larger M values, however, this convergence is much slower, and the analysis is made more difficult by the appearance of a crossover effect, which change the behavior in the small N region, and makes the curves more flat there. While for $M=16$ the crossover size is around $N\sim 10$ (and hence unobservable), for $M=32$ it is at $N\sim 100$, and for $M=48$ it is at $N\sim 250$, showing that the crossover size scales for larger lengths as more and more states are kept.

A possible interpretation of this crossover effect can be obtained by recalling that there are two different sources of errors in the DMRG method (see Sec. III). For small M, this is clearly the ''truncation'' error that dominates. Curves with $M=4,8,16$ in Figs. 3(a,b) basically show the size dependence of this type of error alone. The effect of the ''environment'' error only shows up for large enough M and small enough N values, when the truncation error is strongly reduced. The environment error approaches its saturation earlier than the truncation error, as is seen from the $M=48$ curves, where the environment error dominates. However, since the truncation error increases several orders of magnitude in the small N regime, it always exceeds the environment error for large enough sizes. This produces a rather sharp break in the curves in the log-log plot at the crossover size, such as seen for $M=32$ in the figure.

For comparison, and to reduce the environment error, computations using the *finite lattice algorithm* were also performed. Fixing the chain length at $N=100$, the iteration process was repeated until the desired energies converged. For $\gamma=2$, the relative errors are plotted in Figs. 4(a,b) as a function of the sum of the discarded density matrix eigenvalues $1-P_m$. While there is practically no improvement in the ground-state energy, the first excited-state energy becomes much more precise, when further cycles are carried out, and full convergence is reached only after the $I=3$ iteration. At the critical point $\gamma=1$, δE_{GS} and δE_{1XS} behave similarly: two cycles are needed to get rid of the environment error [Figs. 5(a,b)].

It is seen in the figures that the $I=1$ cycle data (the infinite lattice algorithm results) do not fit onto a straight line on the log-log plot. Points from the fully converged cycles, however, do so nicely. The slope of the fitted line was found to be very close to unity in all cases, indicating that the error is proportional to the discarded weights, i.e.,

$$\delta E = \text{const}(1-P_m), \tag{23}$$

where the constant can depend on the model parameters and the system size. We emphasize, however, that this form only holds for the *converged* energies. Extrapolating the infinite lattice algorithm ($I=1$) data by this formula to the $1-P_m\to 0$ ($M\to\infty$) limit can yield false results.

B. One-point correlation functions

Expectation values of local operators in the ground state were computed using the finite lattice algorithm at a fixed chain length $N=100$. Both $\mathcal{M}_n^x$ and $\mathcal{M}_n^z$ ($n=1,\ldots,100$) were measured, and the errors $\delta\mathcal{M}_n^\alpha \equiv \mathcal{M}_n^\alpha(\text{DMRG})$

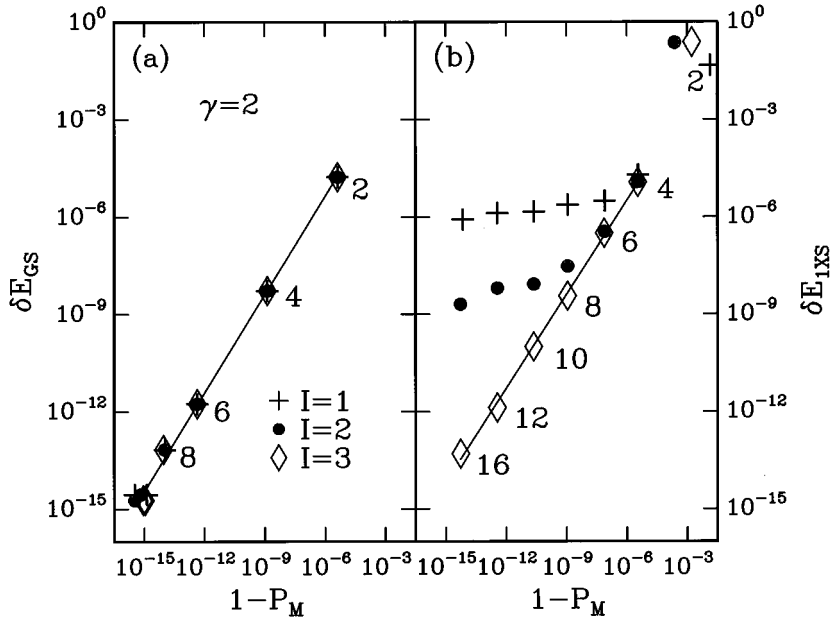

FIG. 4. Relative errors of (a) the ground-state energy, and (b) first excited-state energy as a function of the sum of the discarded density matrix eigenvalues $1-P_m$ for different values of M (shown as labels). Data obtained by the finite lattice algorithm, carrying out the $I=1,2,3$ iteration cycles, and the chain length is fixed at $N=100$. Disordered regime at $\gamma=2$.

$-\mathscr{M}_n^{\alpha}$(exact), $\alpha=x,z$ were calculated. Note that for $\mathscr{M}_n^x$, the exact values are zero, as it was detailed in Sec. II.

At the critical point $\gamma=1$, our results are presented in Figs. 6(a,b). The $I=1$ cycle (infinite lattice algorithm) produces an error which depends significantly on the position in the chain n. Results are more precise around the middle of the system. Note that spatial variations can reach several orders of magnitude for larger M values, as e.g. for the $I=1$, $M=16$ curve in Fig. 6(a). There is also a sudden improvement in accuracy very near to the chain ends, but this is believed to be an anomaly of the ITF model and not a general feature of the DMRG technique. (The exact one-point functions of the model, when open boundary condition is used, show a strong boundary effect close to the ends, and this seems to influence the errors too.)

In the case of $\mathscr{M}_n^z$ [Fig. 6(a)], additional iteration cycles ($I\geqslant 2$) considerably improve the precision by decreasing the environment error. Although some fluctuations may still be present (especially for large M) in the $I=2$ data, the error becomes more or less constant and spatially more homogeneous for $I\geqslant 2$. The convergence found with respect to the number of cycles is similar to that of the energies.

For $\mathscr{M}_n^x$ [Fig. 6(b)], where the exact values of the magnetization are zero, the situation is different. Additional cycles, and increasing the value of M, rather unexpectedly, make the data less precise. The sign of the error also changes: while for the $I=1$ cycle $\delta\mathscr{M}_n^x$ is negative, for $I=3$ it always turns out to be positive. (Note that in the figure the absolute values of the errors are plotted.) The rapid oscillations seen in the $I=2$, $M=8$ curve are due to the fact

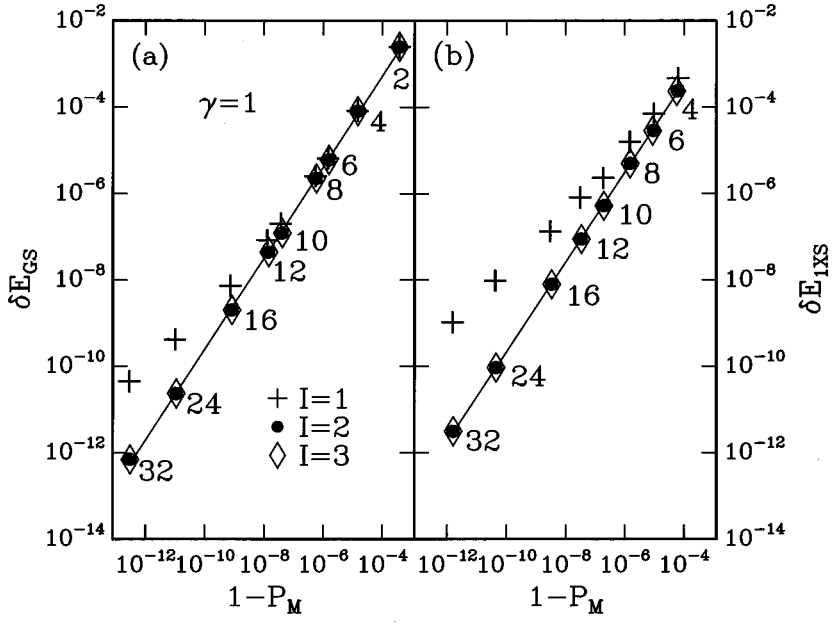

FIG. 5. Same as Fig. 4, but at the critical point $\gamma=1$.

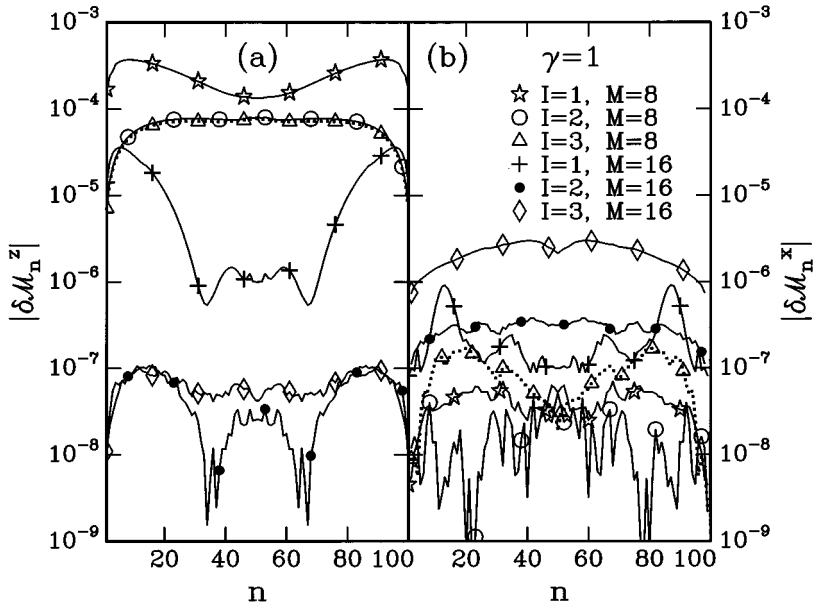

FIG. 6. Errors of the one-point functions (a) $\mathscr{M}_n^z$, and (b) $\mathscr{M}_n^x$ as a function of the position in the chain n. Data obtained by the finite lattice algorithm, carrying out the $I=1,2,3$ iteration cycles, and keeping $M=8$ or 16 states. The chain length is fixed at $N=100$. Critical point $\gamma=1$.

that the error fluctuates between positive and negative values. We believe that for this pathological case the observed errors stem from the numerical inaccuracy of the diagonalization subroutines, and not from the algorithm itself. Test runs on short systems keeping all states in the blocks, i.e., when the DMRG is numerically exact, produced the same qualitative picture of $\delta\mathscr{M}_n^x$.

It might have been thought that monitoring the magnitude of errors of quantities, whose exact results are *a priori* known, like $\mathscr{M}_n^x$ in our case, could yield information on the precision on other, *a priori* not known, quantities, like $\mathscr{M}_n^z$. We see, however, that the errors of the two one-point functions behave completely differently without any obvious correlation, so the knowledge of the accuracy of one of them cannot be used to draw predictions on the other one.

For the $\gamma=2$ case (figure not presented), all the iteration cycles gives the same result for $\mathscr{M}_n^z$. There is practically no n dependence, and the algorithm reaches the border of numerical inaccuracy very soon, in accordance with what was found for the ground-state energy. For $M=8$, the relative errors scatter on the scale of 10^{-9}, and this precision could not be improved by increasing M. The behavior was found to be very similar in the ordered phase, at $\gamma=0.5$, the only difference is that more cycles were needed for the full convergence.

C. Two-point correlation functions

Measurements of the two-point correlation functions were carried out similarly to the one-point correlation functions, at a fixed length $N=100$. Following White's recipe, $\rho_l^\alpha \equiv \rho_{n,n+l}^\alpha$, $\alpha=x,z$, was measured so that the points n and $n+l$ were positioned symmetrically to the middle of the chain.[1] This special allocation of the points assures that, at least for the short-range correlations, end effects are strongly reduced. Although, in most applications the bulk correlation functions are of interest, since our aim was to test the DMRG algorithm itself, we compared the numerical data with the exact finite-lattice results obtained at $N=100$.

At the critical point, $\gamma=1$, the absolute value of the error of the correlation functions $|\delta\rho_l^\alpha| \equiv |\rho_l^\alpha(\text{DMRG}) - \rho_l^\alpha(\text{exact})|$ is plotted in Figs. 7(a,b) for $\alpha=z$ and x. For small M values, the curves are rather smooth with a moderate dependence on l. Convergence with respect to the number of cycles I is reached when the ground-state energy converges. For larger values of M, the errors seem to fluctuate rather irregularly, especially for $|\delta\rho_l^x|$, for which several cusps evolve, where the error rate drops abruptly. This strange feature, however, is once again an artifact of plotting the *absolute value* of the error on a logarithmic scale. For each l where the cusp appears, we found that $\delta\rho_l^\alpha$ changes sign, similarly to the behavior of the corresponding $\mathscr{M}_n^x$ curve, and this sign fluctuation causes the strange-looking shape of the curves.

Disregarding the fact that the sign of the errors is not fixed, there is a clear tendency that in the $I=1$ cycle (infinite lattice algorithm) the long-range correlators are less precise. This is in complete accordance with the behavior of the one-point functions: operators are represented less accurately moving towards the chain ends because of the environment error. More cycles improve the situation, especially for $\delta\rho_l^z$ [Fig. 7(a)], where the errors for large l decrease by 3 orders of magnitude and, quite unexpectedly, the long-range correlators become more precise than the short-range ones. On the other hand, there is no similar change in the tendency of the curves for $\delta\rho_l^x$ [Fig. 7(b)]. Although the improvement is the most significant for large l, long-range correlators remain less accurate.

For the noncritical values $\gamma=2$ and 0.5 (figure not presented), $\delta\rho_l^z$ and $\delta\rho_l^x$ show practically no l dependence. There is only a moderate change in accuracy for very small and very large values of l, but this does not exceed an order of magnitude. The average accuracy of the correlation functions is considerably worse than that of the energies. The limit of the relative precision we could achieve by increasing M was not better than 10^{-9}, similarly to what was found in the case of the one-point functions. The effect of carrying out

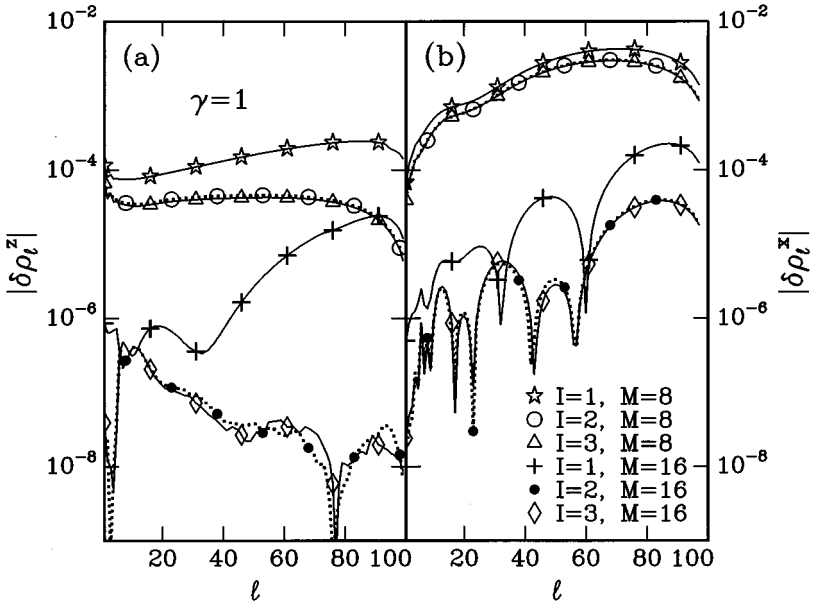

FIG. 7. Errors of the two-point functions (a) ρ_l^z, and (b) ρ_l^x as a function of l. Data obtained by the finite lattice algorithm, carrying out the $I=1,2,3$ iteration cycles, and keeping $M=8$ or 16 states. The chain length is fixed at $N=100$. Critical point $\gamma=1$.

more cycles was also similar, the correlation functions converged exactly when the energies reached their limit values.

V. SUMMARY

In the present paper, we have analyzed in detail the accuracy of White's density-matrix renormalization-group method, by applying it to the one-dimensional Ising model in a transverse field. Due to the exact solvability of this model, the exact and the numerical results could have been directly compared. We varied several parameters, either in the numerical algorithm or in the model, and obtained a rather detailed picture how the accuracy of the DMRG approximation depends on these parameters.

Our main results are summarized as follows.

(i) The DMRG yields an extremely precise value for the ground-state energy, especially when the model is far from the critical point, and the ground state is unique. Excited state energies or the ground-state energy of a critical system can be obtained with much less accuracy.

(ii) Targeting exclusively one of the excited states is, in general, more precise than targeting it together with the ground states or other low-energy states. This, however, can become unstable when the levels are too close to each other, like in the case of asymptotic degeneration of the ground state. When this is expected to happen, more states must be targeted together.

(iii) Carrying out only the $I=1$ iteration cycle (infinite lattice algorithm) leads to a significant ''environment'' error. Its effect is the most pronounced, when lots of states are kept, i.e., when M is large, so the ''truncation'' error is relatively small. The two types of error produce a crossover effect as N increases in the critical case. The environment error dominates in the small N large M regime.

(iv) Although the chain length dependence of the errors is strong in the critical case, both the truncation and the environment errors seem to converge to finite values as N increases. In the practical range of applications $10<N<300$, however, the errors, especially the truncation error, become larger by 2–3 orders of magnitude.

(v) For large M values, the *finite* lattice algorithm ($I\geqslant 2$) improves the results considerably by decreasing the environment error. This is seen not only in the energies, but in the one- and two-point correlation functions. When the data are fully converged (but not after the first $I=1$ cycle), the errors are nicely proportional to the sum of the discarded density matrix eigenvalues $1-P_m$. This fact can be used to make an extrapolation to the $M\rightarrow\infty$ limit.

(vi) Accuracy of the correlation functions is always worse than that of the energies. In the $I=1$ cycle, the error in the representation of the local operators becomes larger as one moves outward from the chain center. When two-point functions are computed in the usual way, i.e., symmetrically to the chain center, this leads to the fact that the long-range correlators are less precise. Additional iteration cycles make the errors smaller and their spatial dependence more homogeneous.

Although the one-dimensional ITF is a rather simple many body system, we believe that most of our findings hold equally well for other, more complex quasi-one-dimensional lattice problems. We hope that the above results contribute to a better understanding of the DMRG procedure, and provide a direct help in optimizing the algorithm in other applications.

ACKNOWLEDGMENTS

The authors would like to thank Jenő Sólyom for encouragement, helpful discussions, and the critical reading of the manuscript. This research was supported in part by the Hungarian Research Fund (OTKA) Grant Nos. 2979, 15870, and by the Swiss National Science Foundation Grant No. 20-37642.93 to Paul Erdös. Ö.L. gratefully acknowledges the hospitality of the Institute of Theoretical Physics of the University of Lausanne, where this work was started.

*On leave from the Research Institute for Solid State Physics, Budapest, Hungary.

[1] S. R. White, Phys. Rev. Lett. **69**, 2863 (1992); Phys. Rev. B **48**, 10 345 (1993).

[2] K. Wilson, Rev. Mod. Phys. **47**, 773 (1975).

[3] R. Chitra, S. Pati, H. R. Krishnamurthy, D. Sen, and S. Ramasesha, Phys. Rev. B **52**, 6581 (1995); K. A. Hallberg, P. Horsch, and G. Martínez, *ibid.* **52**, 719 (1995).

[4] S. R. White and D. A. Huse, Phys. Rev. B **48**, 3844 (1993); U. Schollwöck and T. Jolicoeur, Europhys. Lett. **30**, 493 (1995); S. Qin, T-K. Ng, and Z-B. Su, Phys. Rev. B **52**, 12 844 (1995); R. J. Bursill, T. Xiang, and G. A. Gehring, J. Phys. A **28**, 2109 (1995); S. Östlund and S. Rommer, Phys. Rev. Lett. **75**, 3537 (1995); G. Fáth and J. Sólyom, Phys. Rev. B **51**, 3620 (1995).

[5] R. M. Noack, S. R. White, and D. J. Scalapino (unpublished); A. E. Sikkema and I. Affleck, Phys. Rev. B **52**, 10 207 (1995); S. J. Qin, S. D. Liang, Z. B. Su, and L. Yu, *ibid.* **52**, 5475 (1995); G. Fáth, Z. Domański, and R. Lemański, Phys. Rev. B **52**, 13 910 (1995).

[6] C. C. Yu and S. R. White, Phys. Rev. Lett. **71**, 3866 (1993); E. S. Sørensen and I. Affleck, Phys. Rev. B **51**, 16 115 (1995); (unpublished); W. Wang, S. Qin, Z-Y. Yu, L. Yu, and Z. Su, Phys. Rev. B **53**, 40 (1996).

[7] R. M. Noack, S. R. White, and D. J. Scalapino, Phys. Rev. Lett. **73**, 882 (1994); Europhys. Lett. **30**, 163 (1995); S. R. White, R. M. Noack, and D. J. Scalapino, Phys. Rev. Lett. **73**, 886 (1994); J. Low Temp. Phys. **99**, 593 (1995); C. A. Hayward, D. Poilblanc, R. M. Noack, D. J. Scalapino, and W. Hanke, Phys. Rev. Lett. **75**, 926 (1995).

[8] K. Hallberg, Phys. Rev. B **52**, R9827 (1995).

[9] S. Liang and H. Pang, Phys. Rev. B **49**, 9214 (1994).

[10] A. Drzewiński and F. Daerden, J. Magn. Magn. Mater. **140-144**, 1621 (1995).

[11] G. G. Cabrera and R. Jullien, Phys. Rev. B **35**, 7062 (1987).

[12] E. Lieb, T. Schultz, and D. Mattis, Ann. Phys. (N.Y.) **16**, 407 (1961).

[13] T. W. Burkhardt and I. Guim, J. Phys. A **18**, L33 (1985).

[14] F. Iglói, Phys. Rev. B **48**, 58 (1993); S. R. White and R. M. Noack, Phys. Rev. Lett. **68**, 3487 (1992).

[15] A. Drzewiński and J. M. J. van Leeuwen, Phys. Rev. B **49**, 403 (1994).